

ETTrack: Enhanced Temporal Motion Predictor for Multi-Object Tracking

Xudong Han, Nobuyuki Oishi, Yueying Tian, Elif Ucurum, Rupert Young,
Chris Chatwin, Philip Birch

School of Engineering and Informatic, University of Sussex, Falmer, BN1 9QT, East
Sussex, United Kingdom.

*Corresponding author(s). E-mail(s): P.M.Birch@sussex.ac.uk;
Contributing authors: xh218@sussex.ac.uk;

Abstract

Many Multi-Object Tracking (MOT) approaches exploit motion information to associate all the detected objects across frames. However, many methods that rely on filtering-based algorithms, such as the Kalman Filter, often work well in linear motion scenarios but struggle to accurately predict the locations of objects undergoing complex and non-linear movements. To tackle these scenarios, we propose a motion-based MOT approach with an enhanced temporal motion predictor, ETTrack. Specifically, the motion predictor integrates a transformer model and a Temporal Convolutional Network (TCN) to capture short-term and long-term motion patterns, and it predicts the future motion of individual objects based on the historical motion information. Additionally, we propose a novel Momentum Correction Loss function that provides additional information regarding the motion direction of objects during training. This allows the motion predictor rapidly adapt to motion variations and more accurately predict future motion. Our experimental results demonstrate that ETTrack achieves a competitive performance compared with state-of-the-art trackers on DanceTrack and SportsMOT, scoring 56.4% and 74.4% in HOTA metrics, respectively.

Keywords: Multi-object tracking, Motion model, Kalman filter, Transformer, Temporal convolutional network

1 Introduction

Multi-Object Tracking (MOT) is an important technology in the field of computer vision and plays a significant role in applications such as mobile robotics (Yuan et al., 2022), autonomous driving (Sun et al., 2020), and sports analytics (Zhao et al., 2023). With recent progress in object detection, tracking-by-detection methods (Bewley et al., 2016; Wojke et al., 2017; Du et al., 2023) have become the most popular paradigm. These approaches typically comprise

two subtasks: detecting objects in each frame; and associating them across various frames. The core of the tracking-by-detection paradigm is data association, which relies heavily on the utilization of object appearance and motion information for accuracy. Despite the benefits of employing detection to gain semantic advantages, this reliance poses significant challenges in complex scenarios where objects exhibit similar appearances and object occlusions occur frequently. Therefore, ReID-based MOT methods (Wojke et al., 2017; Du et al., 2023; Fischer et al., 2023), which use a

trained ReID model to extract the appearance features of objects for data association, suffer from degradation of the tracking performance under such conditions. By contrast, motion information becomes relatively reliable in scenarios plagued by similarities in appearance, blurring, and occlusions.

Notably, motion model based MOT approaches(Bewley et al., 2016; Zhang et al., 2022; Cao et al., 2023) utilize a motion predictor to recognize spatial and temporal patterns, thereby predicting future object movements for object association. However, it is still challenging for motion predictors to predict object motion in complex scenarios, such as those involving non-linear movements, diverse poses, and severe occlusions. In this work, our aim is to develop a temporal motion predictor that increases the accuracy of object association and tracking performance.

As the main branch of motion model-based tracking, filtering-based methods widely use the Kalman Filter(Kalman et al., 1960) as a motion predictor with the assumption of constant velocity in both the prediction and filtering processes. The Kalman Filter works well with linear motion, but inaccurately predicts object locations in complex non-linear motion situations. To overcome these limitations, deep-learning-based motion models have been applied to MOT. For example, (Milan et al., 2017; Kesa et al., 2021) adopt Recurrent Neural Networks (RNNs) to predict the object position based on the historical trajectories of objects by exploiting their sequence processing capabilities. (Chaabane et al., 2021) employs a Long Short-Term Memory-based (LSTM) motion model to capture motion constraints by considering the motion information of objects as input. (Xiao et al., 2023) proposes a Transformer-based motion model to capture long-range dependencies for modeling motions. However, these deep-learning-based approaches have two limitations. First, owing to their simple network structure, when utilized in MOT they are unable to effectively handle input sequences with high variability and have difficulty modeling complex and long-range temporal dependencies (Luo et al., 2018). Second, current motion models only consider the historical trajectories of objects as inputs

and lack the capacity to integrate reliable additional information, resulting in unreliable position prediction in complex and non-linear scenes. Nonetheless, integrating additional information is possible, such as the appearance features of objects(Kesa et al., 2021) and the interaction between objects(Han et al., 2023). However, when significant occlusions and predefined actions are present in these scenes(Sun et al., 2022), the performance is compromised.

To mitigate the adverse effects of these limitations, this work proposes two main innovations. We introduce an enhanced temporal motion predictor that integrates a Temporal Transformer model(Vaswani et al., 2017) and a Temporal Convolutional Network (TCN)(Bai et al., 2018) for MOT. The successful application of the Transformer model in Natural Language Processing (NLP) domains(Vaswani et al., 2017; Devlin et al., 2018; Lan et al., 2019) has demonstrated its capability to model long-range temporal dependencies using a powerful self-attention mechanism. We utilize a specialized Temporal Transformer architecture that utilizes only the encoder component of the traditional Transformer model. This design efficiently captures the historical motion patterns of individual objects to predict their motion. The TCN, which employ dilated causal convolution, models human motion to capture basic motion patterns and temporal interdependencies. Furthermore, the TCN can capture the motion patterns of objects on various time scales, particularly short-term minor changes, through the adaptable adjustment of the convolutional kernel size and expansion factor. Integrating the Temporal Transformer and the TCN enables our motion predictor to comprehend both local and global motion information. The TCN excels at capturing fine-grained motion details, while the Temporal Transformer builds upon this to comprehend broader, long-term motion trends.

In addition to the motion predictor, we study the influence of the motion direction of the objects on their predicted positions. In scenarios involving rapid posture changes and swift movements, it is a challenging task for a motion predictor to swiftly acquire and incorporate motion information and make prompt adjustments to motion prediction. Therefore, the efficacy of modeling motion information based on past trajectories is

considerably diminished. During complex movements, the motion direction of an object can shift significantly, making motion direction information a crucial factor in predicting future object motion. We propose a novel loss function called Momentum Correction Loss (MCL), which is employed as a regularizer for the primary motion prediction task. During training, the motion predictor is guided by a loss function that encourages the predicted motion directions to align with the actual motion direction. In MOT tasks, the position of an object is typically represented by a bounding box. In scenarios where the posture of some objects suddenly changes(Sun et al., 2022), we consider not only the motion directions of the center point of the objects but also the motion directions of their four corners. By incorporating additional motion direction information, the model predictor can rapidly adapt to motion variations and predict future motion more accurately. The contributions of this study can be summarized as follows:

1. We propose an enhanced temporal motion predictor that integrates a Temporal Convolutional Network (TCN) and a Temporal Transformer model. It can effectively capture and comprehend objects’ motion patterns to improve object tracking performance.
2. We introduce a novel momentum correction loss function that provides the motion predictor with additional information about the motion direction of objects by correcting the motion direction of objects during learning.
3. We demonstrate that our proposed method achieves competitive performance on challenging datasets, such as DanceTrack (Sun et al., 2022) and SportsMOT (Cui et al., 2023), where non-linear movements, diverse poses, and severe occlusion are present. Furthermore, our method achieves comparable results on MOT17(Milan et al., 2016).

2 Related Works

2.1 Multi-Object Tracking

Multi-Object Tracking methods can be categorized into two types: tracking-by-detection and joint-detection-tracking. Tracking-by-detection methods, such as SORT(Bewley et al., 2016) and DeepSORT(Wojke et al., 2017), first detect

objects and then associate them using appearance and motion information. These methods have long been the dominant paradigm in MOT. Alternatively, joint-detection-tracking methods, such as JDE(Wang et al., 2020) and FairMOT(Zhang et al., 2021), incorporate the detection and ReID model for joint training, offering comparable performance with low computational costs. However, joint-detection-tracking methods may face reduced efficiency owing to conflicts between the detection and tracking optimization goals in their unified network. Additionally, ByteTrack(Zhang et al., 2022) utilizes a simple yet effective data association method BYTE to significantly enhance the tracking accuracy and robustness. Recently, BotSORT(Aharon et al., 2022) with a stronger ReID model outperforms ByteTrack by leveraging both motion and appearance information. Thus, Tracking-by-detection methods demonstrate that a robust detector combined with a simple association approach can attain good tracking results. Therefore, we chose to follow the ByteTrack algorithm replacing the Kalman Filter(Kalman et al., 1960) with a deep-learning-based motion model.

2.2 Motion Model

Several mainstream MOT algorithms(Bewley et al., 2016; Wojke et al., 2017; Cao et al., 2023; Choi, 2015) use motion models. Typically, SORT-series trackers(Bewley et al., 2016; Zhang et al., 2022; Cao et al., 2023) utilize the Bayesian estimation(Lehmann and Casella, 2006) as a motion model to predict the subsequent state by maximizing posterior estimation. For instance, SORT(Bewley et al., 2016) utilizes the classic Kalman Filter(Kalman et al., 1960), assuming linear motion for object estimation, and the Hungarian matching algorithm(Kuhn, 1955) to match predictions and detections. OC.SORT(Cao et al., 2023) enhances robustness in handling occlusions by prioritizing object observations rather than linear state estimations, but it still suffers from long-term occlusion and struggles in recovering lost objects undergoing non-linear motion. However, as has been emphasized, Kalman Filter based methods presuppose a constant motion, which does not accurately describe the change in object positions when undergoing complex interactions within a scene. Therefore, some MOT

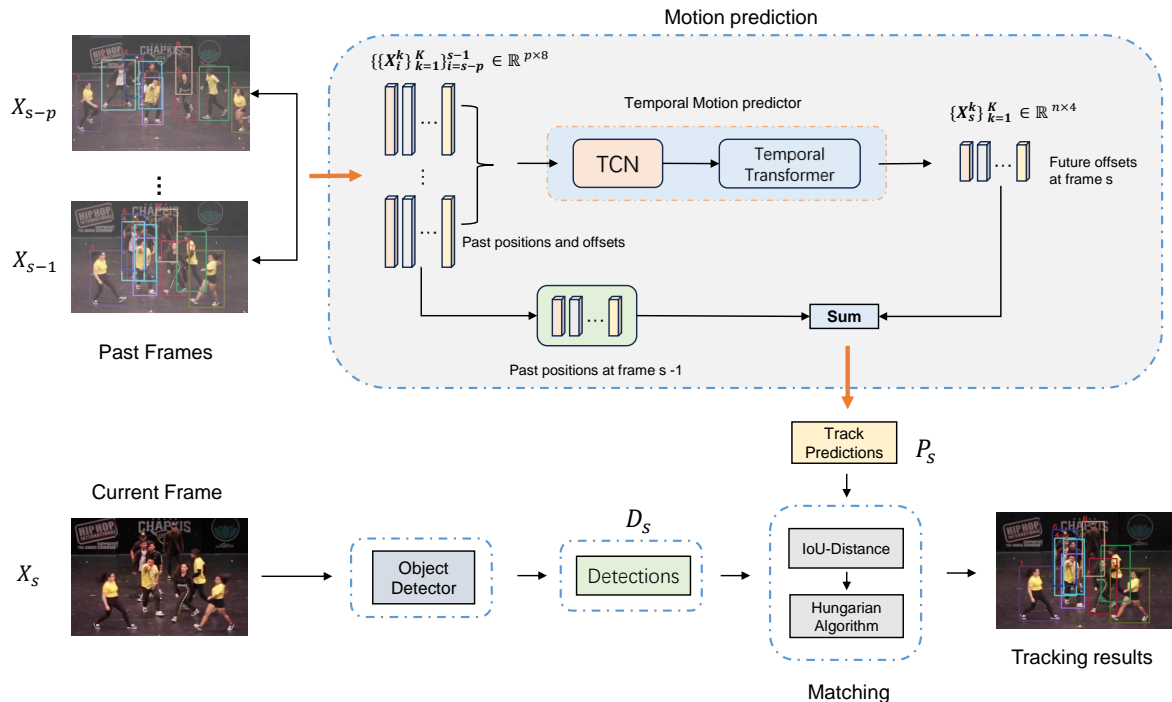


Fig. 1 The pipeline of ETTrack. The historical trajectory of length p is fed into our motion predictor, which predicts the track predictions P_s at the current moment s . By deploying an object detector, detections D_s are obtained. With the track predictions and detections, data association can be accomplished by IoU Distance and Hungarian matching algorithm. Different colors represent different identities in the tracking results

methods introduce deep-learning-based motion models (Milan et al., 2017; Kesa et al., 2021) for non-linear motion modeling. For example, (Milan et al., 2017) presents a novel tracker based on recurrent neural networks (RNNs) for online MOT. (Kesa et al., 2021) proposes a joint learning architecture for improved MOT and trajectory forecasting by leveraging the capabilities of RNNs and adding additional appearance information, thereby surpassing the limitations imposed by using a traditional Kalman Filter. The DEFT algorithm (Chaabane et al., 2021) uses an LSTM to capture the motion constraints of objects. (Xiao et al., 2023) proposes a Transformer-based motion model to capture long-range dependencies for modeling motions. However, these current approaches lack the capacity to model more intricate temporal dependencies and integrate reliable additional information, resulting in inadequate motion prediction capabilities in complex and non-linear scenarios. The proposed method

addresses these limitations and enhances the predictive capabilities.

2.3 Transformer-based Methods

Since the Transformer (Vaswani et al., 2017) has become popular in computer vision, many methods (Meinhardt et al., 2022; Zeng et al., 2022; Sun et al., 2012; Chu et al., 2023; Zhang et al., 2023) for the MOT task have been proposed to leverage its powerful attention mechanism to extract deep representations from both visual information and object trajectories. For example, TrackFormer (Meinhardt et al., 2022) and MOTR (Zeng et al., 2022) extend from Deformable DETR (Zhu et al., 2020). They utilize both track queries and standard detection queries to predict object bounding boxes and associate the same objects in subsequent frames. TransTrack (Sun et al., 2012) employs only Transformers as its feature extractor and propagates track queries once to obtain the position of objects in the subsequent

frame. TransMOT(Chu et al., 2023) uses convolutional neural networks (CNNs) as a detector to extract features and employs spatial-temporal transformers to learn an affinity matrix. Recently, MOTRv2(Zhang et al., 2023) combines a separate detector with MOTR(Zeng et al., 2022) to address the conflict between the detection and association. However, Transformer-based methods require extensive training time and computational resources, which prevents them from achieving real-time capability. In contrast, the proposed method utilizes the powerful temporal dependency modeling capabilities of a Transformer to model the movement of objects. In addition, the ETTrack method relies solely on trajectory data as input, which significantly decreases the computation time required for motion model inference during the runtime.

3 Method

In this work, we propose an enhanced temporal motion predictor that effectively utilizes motion cues to track objects with complex motion patterns. Our primary objective is to achieve precise estimates of non-linear uncertainties by integrating a Temporal Transformer with a Temporal Convolutional Network (TCN) that surpasses the performance of some deep-learning-based motion models. In addition, we propose a momentum correction loss function to enhance the motion predictor by using motion direction information. Section 3.2.1 and Section 3.2.2 describe the Temporal Transformer and the Temporal Convolutional Network (TCN) respectively, while Section 3.2.3 introduces the concept of momentum correction loss function.

3.1 Problem Formulation

The trajectory of an individual object i contains a sequence of bounding boxes $\mathbf{B} = \{b_{t_1}, b_{t_2}, \dots, b_{t_N}\}$, where t stands for the timestamp, and N is the total number of frames. The bounding boxes are represented as $b=(x, y, w, h)$. The aim of MOT is to assign a unique identifier to all the frame-wise bounding boxes. This assignment aims to establish a comprehensive association between all the bounding boxes.

Our goal is to create a motion predictor that predicts the locations of objects. When the

historical trajectory length of objects is set to p , the historical trajectory of objects can be denoted as a sequence $\mathbf{X} \equiv \{\{X_i^k\}_{k=1}^K\}_{i=s-p}^{s-1} \equiv \{\{X_{s-p}^k\}, \{X_{s-p+1}^k\}, \dots, \{X_{s-1}^k\}\} \in \mathbb{R}^{p \times 8}$, where K is the total number of objects across all frames and s is the frame index. The object k at the moment $s - 1$ is denoted by $\mathbf{X}_{s-1}^k = (x_{s-1}^k, y_{s-1}^k, w_{s-1}^k, h_{s-1}^k, \Delta x_{s-1}^k, \Delta y_{s-1}^k, \Delta w_{s-1}^k, \Delta h_{s-1}^k)$, where (x_{s-1}^k, y_{s-1}^k) are the center coordinate of the corresponding bounding box, (w_{s-1}^k, h_{s-1}^k) stand for the width and height of the bounding box, respectively, and $\mathbf{V}_{s-1}^k = (\Delta x_{s-1}^k, \Delta y_{s-1}^k, \Delta w_{s-1}^k, \Delta h_{s-1}^k)$ is the velocity of the object. These historical trajectories are fed into the motion predictor to predict the velocity $\mathbf{V}_s^k = (\Delta x_s^k, \Delta y_s^k, \Delta w_s^k, \Delta h_s^k)$ at the current moment s .

Predicting offsets (i.e., position changes) between successive frames offers two advantages for motion prediction. First, predicting position changes simplifies the overall prediction task because it involves analyzing relative movements, which typically exhibit less variation and more predictable patterns than the absolute positions. By focusing on relative movements, the complexity of the prediction process is reduced. Second, our motion predictor becomes less sensitive to specific starting points or trajectory shapes. This advantage enables the motion predictor to effectively capture the underlying movement dynamics, thereby improving its ability to generalize across different scenarios and unseen data.

To obtain the predicted position at the current moment s , the motion predictor adds bounding boxes $\{X_{s-1}^k\}_{k=1}^K$ from the last frame to the predicted velocities to generate the predicted current bounding boxes $\mathbf{X}_s^k = \{x_s^k, y_s^k, w_s^k, h_s^k\} = \{x_{s-1}^k + \Delta x_s^k, y_{s-1}^k + \Delta y_s^k, w_{s-1}^k + \Delta w_s^k, h_{s-1}^k + \Delta h_s^k\}$. The overall framework of the motion predictor is illustrated in Fig. 1.

3.2 Motion Predictor

The MOT task requires identification of the spatial and temporal locations of objects, specifically their trajectories. It has been demonstrated that the Temporal Transformer can capture global

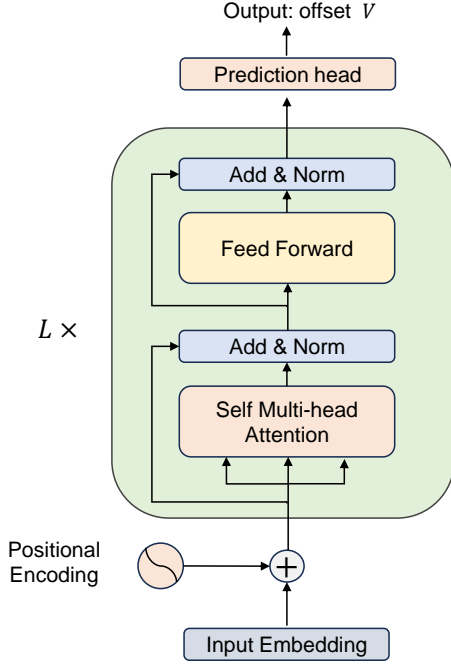


Fig. 2 The network structure of Temporal Transformer in the motion predictor

temporal dependencies and comprehend the overall context of motion sequences, offering a comprehensive perspective of long-range motion interactions and patterns. Moreover, the Temporal Convolutional Network (TCN)(Bai et al., 2018) has proven effective in identifying complex local temporal dependencies in motion sequences, resulting in precise analysis of short-term motion patterns. Thus, the integration of the Temporal Transformer and TCN allows the model to provide a comprehensive understanding of the motion patterns.

3.2.1 Temporal Transformer

The Temporal Transformer is designed to effectively capture the long-term historical motion patterns of individual objects. This is achieved by utilizing a standard transformer encoder, which comprises a multi-head self-attention (MHSA) mechanism. The MHSA enables the encoder to consider various aspects of the trajectory sequence and identify the most critical features for predicting the future positions of objects. The structure of the Temporal Transformer is shown in Fig. 2.

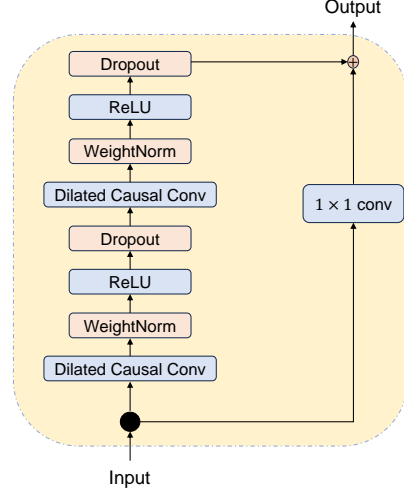


Fig. 3 Structure of the TCN

In the Temporal Transformer, the input sequence of token T is the output of the Temporal Convolutional Network. The self-attention of the temporal transformer can learn the query matrix $Q = f_Q(T)$, key matrix $K = f_K(T)$, and value matrix $V = f_V(T)$. Self-attention of a single head is calculated as:

$$Attention(Q, K, V) = \frac{\text{softmax}(QK^T)}{\sqrt{d_k}}V, \quad (1)$$

where $\frac{1}{\sqrt{d_k}}$ accounts for the numerical stability of self-attention. In Eq.1, softmax is the distribution function, which depends on the properties of the model. Utilizing multiple matrices for attention recurrence allows for a more effective handling of complex temporal dependencies. This is achieved through the implementation of multi-head attention, which involves embedding the outputs of multiple self-attention mechanisms. This method enables the model to simultaneously consider information from various subspaces of representation at different positions, thereby enhancing its ability to process and understand complex information. With n heads, the multi-head attention can be represented as:

$$Multi\ Attention = f_h(Attention(Q_i, K_i, V_i)_{i=1}^n), \quad (2)$$

where f_h is a fully connected feed-forward network. A positional encoding method is implemented to provide the Transformer encoder with

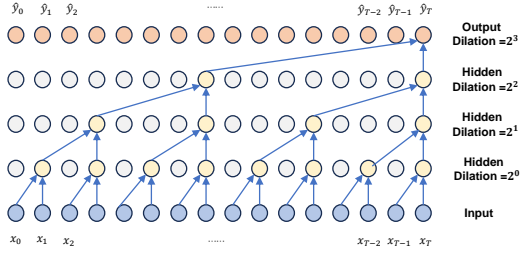


Fig. 4 visualization of a stack of dilated causal convolutions ($K = 7$, Dilation = $[2^0, 2^1, 2^2, 2^3]$)

positional information and to enable the attention layer to perform multi-head self-attention on the output of the TCN. Finally, the output of n heads is cascaded and fed into f_h to obtain the Transformer output. The temporal Transformer is an important implementation of the Transformer model for modeling object motion by processing sequential data. In our experiments, we demonstrate that the temporal Transformer can efficiently capture the temporal interdependencies within the input trajectory sequence.

3.2.2 Temporal Convolutional Network

The Temporal Convolutional Network (TCN) is an innovative structure optimized for sequential data processing that effectively addresses temporal dependencies using a deep learning approach. A standard TCN is composed of multiple TCN blocks, each designed to capture temporal patterns and ensure robust feature representation. Details of the TCN are shown in Fig. 3. Each TCN block consists of successive layers, beginning with a pair of causal convolutions. These convolutions ensure that the model’s predictions are solely dependent on past and present information rather than future data. Although causal convolutions have been shown to be effective in modeling short-term dependencies, they have limitations in modeling long-term dependencies because of their limited receptive fields. To enhance the capacity of the TCN to capture longer temporal interdependencies, we can either increase the network depth or the filter size. However, this results in higher computational complexity. Unlike causal convolution, which can only broaden its receptive field by increasing its kernel size or adding more layers, dilated causal convolution employs dilation factors, represented by $dil \in F$, to enlarge its

receptive field. The dilation factor, denoted by dil , can be exponentially increased, as shown in Fig. 4. Using dilated causal convolution, we can calculate the feature map f as follows:

$$f(t) = (I *_{dil} W)(t) \sum_{i=0}^{K-1} w(i)I(t - idil), \quad (3)$$

where I is the input, W represents the filter, and K is the filter size. By stacking these convolutions, a TCN can expand its receptive field and effectively capture longer dependencies. Following dilated causal convolution, two layers of non-linearity are introduced using the ReLU activation function. This non-linearity is crucial for the model to capture complex patterns and relationships in data. Weight normalization is added to the one-dimensional convolutions to improve the training stability and speed. In addition, a dropout block is added after each activation function. Finally, a residual connection is integrated into the layer to enhance the predictive performance of the model. Residual blocks (Zagoruyko and Komodakis, 2016) equipped with identity mapping can be denoted as:

$$T_{j+1} = T_j + \mathcal{R}(T_j, W_j), \quad (4)$$

Where T_j and T_{j+1} represent the input and output of the $(j+1)$ th TCN block, respectively, W_j is the trainable parameter matrix of the residual blocks, and $\mathcal{R}(\cdot)$ denotes a residual function.

Although the TCN can be designed to enhance the capacity to model long-term dependencies using dilated causal convolution, it is equally optimized for modeling short-term dependencies, allowing it to accurately capture local patterns and dynamics in sequence data. The TCN effectively mitigates the limitations of the Temporal Transformer in modeling short-term dependencies, when the tracking task is particularly dependent on localized features in the short term. Moreover, compared with the Temporal Transformer, which requires complex self-attention computation, the TCN typically has a simpler model structure. This not only alleviates computational demands, but also allows TCN models to accomplish the training and inference phases more rapidly in real-world scenarios.

3.2.3 Momentum Correction Loss (MCL)

To enhance the motion predictor model and obtain more reliable future predictions, we incorporate contextual information, such as motion direction. We propose a novel loss called momentum correction loss, which serves as a regularizer for the motion prediction loss. By integrating both the trajectory prediction loss and momentum correction loss, we can effectively train the motion predictor model. The proposed momentum correction loss is shown in Fig. 5. Given two points (x_1, y_1) and (x_2, y_2) , the motion direction is denoted by:

$$\theta = \arctan\left(\frac{y_1 - y_2}{x_1 - x_2}\right). \quad (5)$$

In MOT, the position of an object is typically represented by a bounding box. To adjust to sudden pose changes and swift movements, the predicted object motion direction can be represented as $\theta_p = \{\theta_c, \theta_{lt}, \theta_{rt}, \theta_{lb}, \theta_{rb}\}$, where $\{\theta_c\}$ is the motion direction at the center point and $\{\theta_{lt}, \theta_{rt}, \theta_{lb}, \theta_{rb}\}$ represent the motion direction at the four corners of the object. The real object motion direction can also be denoted as $\theta_t = \{\theta'_c, \theta'_{lt}, \theta'_{rt}, \theta'_{lb}, \theta'_{rb}\}$. In general, the direction of motion of the center point of an object represents the overall direction of motion. In scenarios where the posture of some objects suddenly changes (Sun et al., 2022), it is necessary to consider not only the direction of motion of the center point of an object but also the direction of motion of the four corners of the bounding box. As illustrated in Fig. 5, we can capture more pose changes using the four corners of the bounding box. Thus, the momentum correction loss can be calculated as:

$$\mathcal{L}_{MCL} = \frac{1}{5} \sum_i |\theta_i - \theta'_i|, i \in (c, lt, rt, lb, rb). \quad (6)$$

3.3 Training and Inference

Training. In the training phase, we train the motion predictor by utilizing the historical positions of n frames and predict the object positions of the subsequent frames. We use the L1 loss function as the prediction loss to supervise the training process and improve the capacity to address outliers. Specifically, given the predicted offset $\hat{\mathbf{V}} =$

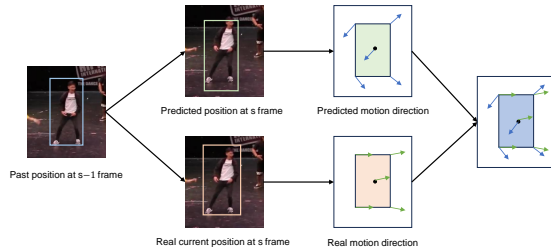


Fig. 5 Illustration of momentum correction loss. We obtain the predicted and actual motion directions, which are represented by the blue and green arrows, respectively. Subsequently, we calculate the angular difference between the predicted and actual motion directions to obtain the momentum correction loss

$\{\hat{v}_x, \hat{v}_y, \hat{v}_w, \hat{v}_h\}$, and the corresponding attributes of the ground truth \mathbf{V} , the prediction loss \mathcal{L}_{pred} is obtained by:

$$\mathcal{L}_{pred}(\hat{\mathbf{V}}, \mathbf{V}) = \sum_i |\hat{v}_i - v_i|, i \in (x, y, w, h). \quad (7)$$

The final loss function sums both the motion prediction loss \mathcal{L}_{pred} and momentum correction loss \mathcal{L}_{MCL} :

$$\mathcal{L}_{final} = \mathcal{L}_{pred} + \beta \mathcal{L}_{MCL}, \quad (8)$$

where β is a crucial hyper-parameter that determines the extent to which the momentum correction loss function is influential. It is worth noting that additional direction information is required only during the training phase. By contrast, during the prediction phase, the model relies solely on the observed trajectory to predict the future trajectory.

4 Experiments

4.1 Datasets and Evaluation Metrics

Inference. Our motion predictor is applied to the ByteTrack (Zhang et al., 2022) platform, which introduces a two-step association algorithm that utilizes object detection thresholds to track every detection box using tracklets and recovers occluded objects based on similarities. We use the motion predictor to output the prediction boxes P_s in the current frame. By utilizing a YOLOX (Ge et al., 2021) detector, the detection boxes D_s are obtained in the current frame. ByteTrack’s association algorithm employs the Hungarian algorithm to assign detections to tracklets based on the

Algorithm 1 Pseudo-code of ETTrack

Input: A video sequence V ; object detector \mathbf{D} ; motion predictor \mathbf{T} ; detection score threshold τ

Output: Tracks \mathcal{T} of the video

```
1: initialization:  $\mathcal{T} \leftarrow \emptyset$ 
2: for frame  $f$  in  $V$  do
3:   /*Detection */
4:    $D_f \leftarrow \mathbf{D}(f)$ 
5:    $D_{high} \leftarrow \emptyset$ 
6:    $D_{low} \leftarrow \emptyset$ 
7:   for  $d$  in  $D_f$  do
8:     if  $d.score \geq \tau$  then
9:        $D_{high} \leftarrow D_{high} \cup \{d\}$ 
10:    else
11:       $D_{low} \leftarrow D_{low} \cup \{d\}$ 
12:    end if
13:  end for
14:  /*motion predictor */
15:  for  $trks$  in  $\mathcal{T}$  do
16:     $trks \leftarrow \mathbf{T}(trks)$ 
17:  end for
18:  /*first association */
19:  Associate  $\mathcal{T}$  and  $D_{high}$  using IOU
20:   $D_{reman} \leftarrow$  remaining detected boxes from  $D_{high}$ 
21:   $\mathcal{T}_{reman} \leftarrow$  remaining predicted boxes from  $\mathcal{T}$ 
22:  /*second association */
23:  Associate  $\mathcal{T}_{reman}$  and  $D_{low}$  using IOU
24:   $\mathcal{T}_{re-reman} \leftarrow$  remaining predicted boxes from  $\mathcal{T}_{reman}$ 
25:  /*delete unmatched tracks */
26:   $\mathcal{T} \leftarrow \mathcal{T} \setminus \mathcal{T}_{re-reman}$ 
27:  /*initialize new tracks */
28:  for  $d$  in  $D_{reman}$  do
29:     $\mathcal{T} \leftarrow \mathcal{T} \cup \{d\}$ 
30:  end for
31: end for
32: Return  $\mathcal{T}$ 
```

Intersection-over-Union (IoU) between P_s and D_s . These successfully associated detection boxes are incorporated into the historical trajectories for updates, and the unassigned detections are then initialized as new trajectories. For inactive trajectories, our motion predictor continues to generate prediction boxes, that are subsequently appended to trajectories to facilitate model inference. When detections are reconnected to these inactive trajectories, the inactive trajectories may also be retracked. If the inactive time exceeds a given threshold, these preserved prediction boxes are deleted. The pseudo-code of ETTrack is shown in Algorithm 1.

Datasets. To conduct a comprehensive evaluation of our method, we performed experiments on various MOT benchmarks including DanceTrack (Sun et al., 2022), SportsMOT (Cui et al., 2023) and MOT17 (Milan et al., 2016). MOT17 is a widely used foundational benchmark in MOT, in which the motion of pedestrians is mostly linear. In contrast, the SportsMOT dataset captures the intricate motions and similar appearances of athletes in sports scenes, incorporating videos from high-profile events, such as the Olympic Games and NBA, thereby demanding high tracking precision. The DanceTrack dataset presents a particularly complex challenge in terms of object tracking. This is because it consists of objects that look very similar to each other, frequently become occluded from view, and exhibit unpredictable movement patterns. Consequently, it is challenging for any tracking algorithm to conclusively demonstrate its ability to handle complex scenarios effectively. Our aim is to propose a motion predictor that can effectively improve the tracking performance in challenging situations, particularly when the Kalman Filter fails under diverse scenarios. SportsMOT and DanceTrack are ideal datasets for evaluating the tracking performance.

Metrics. To evaluate our algorithm, we adapt HOTA (Luiten et al., 2021) as the primary metric. HOTA combines several sub-metrics and provides a balanced view by considering both detection and association accuracy. In addition to HOTA, we also used other CLEAR metrics (Bernardin and Stiefelwagen, 2008), such as MOTA, FP, FN, IDs, etc., and IDF1 (Ristani et al., 2016). MOTA is computed based on FP, FN and IDs and is affected by the detection performance. IDF1 evaluates identity preservation ability and is used to measure association performance. These metrics are widely used to effectively evaluate the algorithm performance.

4.2 Implementation Details

We train the motion predictor solely on the corresponding tracking datasets, without integrating any external samples. In the experiments, we use the publicly available YOLOX (Ge et al., 2021) detector weights developed by ByteTrack (Zhang et al., 2022) for a fair comparison. For the motion predictor, a TCN is employed to encode the past trajectory into a 32-dimensional vector. The TCN

Table 1 Comparison of our method with start-of-the-art MOT algorithms on the DanceTrack test sets

Tracker	HOTA \uparrow	DetA \uparrow	AssA \uparrow	MOTA \uparrow	IDF1 \uparrow
CenterTrack(Zhou et al., 2020)	48.1	86.8	78.1	22.6	35.7
FairMOT(Zhang et al., 2021)	39.7	82.2	66.7	23.8	40.8
QDTrack(Fischer et al., 2023)	45.7	83	72.1	29.2	44.8
TransTrack(Sun et al., 2012)	45.5	88.4	75.9	27.5	45.2
TraDes(Wu et al., 2021)	43.3	86.2	74.5	25.4	41.2
GTR(Zhou et al., 2022)	48	84.7	72.5	31.9	50.3
MORT(Zeng et al., 2022)	54.2	79.7	73.5	40.2	51.5
MotionTrack(Xiao et al., 2023)	52.9	91.3	80.9	34.7	53.8
SORT(Bewley et al., 2016)	47.9	91.8	72	31.2	50.8
DeepSORT(Wojke et al., 2017)	45.6	87.8	71	29.7	47.9
ByteTrack(Zhang et al., 2022)	47.3	89.5	71.6	31.4	52.5
OC_SORT(Cao et al., 2023)	55.1	89.4	80.3	38	54.2
ETTrack(ours)	56.4	92.2	81.7	39.1	57.5

The best results of methods are marked in bold
Methods in bottom block use the same YOLOX detector

Table 2 Comparison of our method with start-of-the-art MOT algorithms on the SportsMOT test sets

Tracker	HOTA \uparrow	IDF1 \uparrow	AssA \uparrow	MOTA \uparrow	DetA \uparrow	LocA \uparrow	IDs \downarrow	Frag \downarrow
FairMOT(Zhang et al., 2021)	49.3	53.5	34.7	86.4	70.2	83.9	9928	21673
QDTrack(Fischer et al., 2023)	60.4	62.3	47.2	90.1	77.5	88	6377	11850
CenterTrack(Zhou et al., 2020)	62.7	60	48	90.8	82.1	90.8	10481	5750
TransTrack(Sun et al., 2012)	68.9	71.5	57.5	92.6	82.7	91	4492	9994
BoT-SORT(Aharon et al., 2022)	68.7	70	55.9	94.5	84.4	90.5	5729	5349
ByteTrack(Zhang et al., 2022)	62.8	69.8	51.2	94.1	77.1	85.6	3267	4499
OC_SORT(Cao et al., 2023)	71.9	72.2	59.8	94.5	86.4	92.4	3093	3474
ETTrack	72.2	72.5	60.1	94.9	86.9	92.5	4075	5279
*ByteTrack(Zhang et al., 2022)	64.1	71.4	52.3	95.9	78.5	85.7	3089	4216
*MixSort_Byte(Cui et al., 2023)	65.7	74.1	54.8	96.2	78.8	85.7	2472	4009
*OC_SORT(Cao et al., 2023)	73.7	74	61.5	96.5	88.5	92.7	2728	3144
*MixSort_OC(Cui et al., 2023)	74.1	74.4	62	96.5	88.5	92.7	2781	3199
*ETTrack	74.3	74.5	62.1	96.8	88.8	92.8	3862	4298

The best results of methods are marked in bold
Methods in middle and bottom block use the same YOLOX detector
Methods with * show that their YOLOX detectors are trained on the SportsMOT train and validation sets

comprises 4 TCN blocks. Moreover, a dropout ratio of 0.1 is implemented during data processing. It is worth noting that all the Temporal Transformer layers accept inputs with a feature size of 32. The Temporal Transformer includes 6 layers, and the multi-head self-attention uses 8 heads. We optimize the network using the Adam algorithm (Kingma and Ba, 2014) algorithm with a learning rate of 0.0015 and a batch size of 16 for 50 epochs. The maximum historical trajectory length p is set to 10. On the training datasets, we conduct hyper-parameter optimization of β . We achieve best tracking results using $\beta = 0.3$ on the

DanceTrack validation sets. All the experiments are conducted using a GeForce RTX 3090 GPU.

4.3 Benchmark Evaluation

Here, we present benchmark results for multiple datasets, such as DanceTrack, SportsMOT, and MOT17. All these methods use the same detection results.

DanceTrack. To demonstrate the performance of ETTrack with non-linear object motion and diverse scenarios, the results for the DanceTrack dataset are presented in Table 1. The performance of our method is tested on the DanceTrack test sets. The results demonstrate that

Table 3 Tracking performance of investigated algorithms on MOT17 dataset

Tracker	HOTA \uparrow	MOTA \uparrow	IDF1 \uparrow	FP \downarrow	FN \downarrow	IDs $\downarrow\downarrow$	AssA \uparrow	AssR \uparrow
FairMOT(Zhang et al., 2021)	59.3	73.7	72.3	27500	117000	3,303	58.0	63.6
QDTrack(Fischer et al., 2023)	53.9	68.7	66.3	26600	147000	3,378	52.7	57.2
TransTrack(Sun et al., 2012)	54.1	75.2	63.5	50200	864000	3,603	47.9	57.1
TransCenter(Xu et al., 2023)	54.5	73.2	62.2	23100	124000	4,614	49.7	54.2
MORT(Zeng et al., 2022)	57.2	71.9	68.4	21100	136000	2,115	55.8	59.2
TransMOT(Chu et al., 2023)	61.7	76.7	75.1	36200	93200	2,346	59.9	66.5
GTR(Zhou et al., 2022)	59.1	75.3	71.5	26800	110000	2,859	61.6	-
ByteTrack(Zhang et al., 2022)	63.1	80.3	77.3	25500	83700	2,196	62.0	68.2
StrongSORT(Du et al., 2023)	63.5	78.5	78.3	-	-	1,446	63.7	-
OC_SORT(Cao et al., 2023)	63.2	78.0	77.5	15100	108000	1,950	63.2	67.5
ETTrack	61.9	79.0	75.9	23100	93300	2,118	60.5	67.0

The best results of methods are marked in bold

Methods in bottom block use the same YOLOX detector

ETTrack performs competitively compared with the other methods. Specifically, ETTrack achieved 56.4% HOTA, 92.2% DetA and 57.5% IDF1, which is better than the OC_SORT method with an enhanced Kalman Filter and recovery strategy. It is noteworthy that a significant gain of 3.4% is observed in the IDF1 score, which assesses the performance of association accuracy. These experimental results provide convincing evidence that our method outperforms SORT-like algorithms (Bewley et al., 2016; Zhang et al., 2022; Cao et al., 2023) that rely on the standard Kalman Filter. Our motion model has proven to be effective for modeling the temporal motion patterns of objects and more robust solution than SORT-like algorithms in non-linear and complex scenarios.

SportsMOT. To further evaluate the performance of ETTrack in non-linear scenarios, we conduct experiments on the SportsMOT benchmark. All methods used the same YOLOX detector trained on the SportsMOT training sets with or without validation sets for a fair comparison. As shown in Table 2, these methods with * show that their YOLOX detectors are trained on SportsMOT train and validation sets. The evaluation results presented in Table 2 show that ETTrack achieves 74.3% in HOTA, 74.5% in IDF1, 62.1% in AssA, 96.8% in MOTA, and 88.8% in DetA. Compared with MixSort_OC(Cui et al., 2023) that designs appearance based association to enhance OC_SORT, our method still outperforms it. Specifically, ETTrack outperforms ByteTrack by up to 10.2% in HOTA and 3.1% in IDF1. Our method has shown a significant advantage

in terms of object instance association, as evidenced by its performance in the HOTA and IDF1 metrics. These results indicate the effectiveness of ETTrack in dealing with non-linear motions.

MOT17. Table 3 presents the tracking performance on the test set of MOT17 to validate the generalizability of the proposed motion model, which covers linear object motion. The results show that although our method achieves results comparable to existing benchmarks, it slightly underperforms relative to the current state-of-the-art methods. Given that the video sequences in MOT17 are captured under varying resolutions and diverse lighting conditions, detection emerges as a crucial element that significantly influences tracking performance. It is worth noting that although MOT17 is specifically designed to track pedestrians in scenarios where motion patterns are generally linear, our approach still achieves comparable performance with advanced methods. Thus, ETTrack consistently demonstrates robust generalizability.

4.4 Ablation Study

A series of ablation studies are conducted on the validation set of the DanceTrack to assess the impact of model components, momentum correction loss, and some hyper-parameters on our proposed method.

Impact of motion modeling. To assess the effectiveness of our motion predictor, we conduct a comparative study using various existing motion models. We employ diverse motion models to incorporate temporal dynamics in the tracking process, as shown in Table 4. Obviously, the

Table 4 Comparison of different motion models on the DanceTrack validation sets

Tracker	HOTA↑	MOTA↑	DetA ↑	AssA↑	IDF1↑
No motion	44.7	87.3	79.6	25.3	36.8
Kalman Filter	46.8	87.5	70.2	31.3	52.1
LSTM	51.2	87.1	76.7	34.3	51.6
Vanilla Transformer	51.9	89.3	78.3	35.5	52.7
Ours	53.3	90.0	78.5	36.3	54.0

The best results are marked in bold

Table 5 Evaluation of different model components

	HOTA↑	MOTA↑	DetA ↑	AssA↑	IDF1↑
W/o TCN	52.2	89.8	78.7	35.7	53.0
Ours	53.3	90.0	78.5	36.3	54.0

"W/o" means that the TCN is removed from the motion predictor

The best results are marked in bold

Table 6 Comparison with/without MCL

	HOTA↑	MOTA↑	DetA ↑	AssA↑	IDF1↑
W/o MCL	52.5	89.9	78.6	35.1	53.1
Ours	53.3	90.0	78.5	36.3	54.0

"W/o" means that the no motion direction information is input to motion predictor

The best results are marked in bold

Kalman Filter and LSTM surpass the IoU association method, demonstrating the considerable potential of motion models in tracking objects, especially when appearance information is unreliable. As shown in Table 4, our method has a significant advantage over the Kalman Filter, LSTM(Chaabane et al., 2021) and Vanilla Transformer(Vaswani et al., 2017), as measured by the HOTA and IDF1. Our motion predictor outperforms the Kalman Filter, which relies on linear motion, by up to 6.5% in HOTA and 1.9% in IDF1. Furthermore, as a deep learning-based motion predictor, our method outperforms Transformer, especially in HOTA and IDF1. Since our motion predictor Integrates TCN and Temporal Transformer models, it can learn motion patterns more comprehensively and predict object positions more accurately.

Impact of model components We conduct an ablative experiment to assess the impact of the core components on our proposed model. Specifically, the TCN is deactivated in our motion

Table 7 Evaluation of p on the DanceTrack validation sets

p	HOTA↑	MOTA↑	DetA ↑	AssA↑	IDF1↑
5	51.5	89.9	77.8	35.1	52.1
8	53.1	89.9	78.2	35.5	53.4
10	53.3	90.0	78.5	36.3	54.0
13	53.2	90.0	78.4	36.4	53.8
15	52.9	90.1	78.1	36.2	53.1

The best results are marked in bold

predictor to examine the resulting changes in the tracking performance. As shown in Table 5, when the TCN is removed from the motion predictor, the HOTA and IDF1 decreased by 1.1% and 1.0%, respectively. As previously discussed, TCN demonstrates strong capability for modeling short-term dependencies and commendable proficiency in capturing long-term dependencies. This capability effectively mitigates the limitations of the Temporal Transformer in modeling short-term dependencies, which are crucial for recognizing the localized features of temporal significance. The results of these experiments demonstrate that the integration of the TCN can effectively improve the prediction performance of the Temporal Transformer by extracting temporal features.

Impact of the Momentum Correction Loss An ablation study examines how the momentum correction loss Eq. 8 behaves, as summarized by the results shown in Table 6. We measure the tracking performance when momentum correction loss is used to train the motion predictor. HOTA and IDF1 levels increase by 0.8% and 0.9%, respectively. The results demonstrate the impact of utilizing the motion direction information in future motion prediction models. There are many sudden changes in pose and swift movements in datasets such as DanceTrack, which makes predictions that rely on past trajectories insufficient. Our future research will explore additional possibilities for incorporating more information into motion prediction.

Impact of historical trajectory length To demonstrate how the tracking performance is affected by the length of the historical trajectory, we evaluate our proposed method at different p values. The results, as listed in Table 7, indicate that a very small historical trajectory length fails to provide sufficient information, resulting in unreliable predictions. Our results indicate that



Fig. 6 Qualitative comparison of OC_SORT and ETTrack (Ours). OC_SORT leads to ID switch due to non-linear motion or severe occlusion, but ETTrack still maintains the identity. Each row shows the results’ comparison for one sequence. Specifically, the problem occurs with OC_SORT’s objects: (a) ID switch between frame #240 and #265; (c) ID switch between frame #315 and #332; (f) ID switch between frame #132 and #146

Table 8 Evaluation of β in Eq. 8

β	HOTA \uparrow	MOTA \uparrow	DetA \uparrow	AssA \uparrow	IDF1 \uparrow
0	52.2	89.9	78.7	35.5	53.1
0.1	52.6	89.9	78.6	35.6	53.3
0.2	52.9	90.1	78.9	36.0	53.7
0.3	53.3	90.0	78.5	36.3	54.0
0.4	52.7	89.8	78.5	36.2	53.5
0.5	51.7	89.8	78.6	35.6	52.9

The best results are marked in bold

extending the historical trajectory length provides a more comprehensive analysis of object motion. However, a very large historical trajectory length tends to provide a considerable degree of noise, which in turn negatively affects the tracking performance. Therefore, we selected T to be 10, which accounts for 0.5 seconds of the object’s historical trajectory, based on a video frame rate of 20 FPS. The results presented in Table 7 demonstrate the significance of choosing an appropriate historical trajectory length to achieve superior performance in object-tracking tasks.

Impact of the weight of the Momentum Correction Loss Finally, we also explore the effect of the hyper-parameter β , which determines the degree to which the momentum correction loss affects the final objective function. As shown in Table 8, the best results are obtained on the DanceTrack validation sets when β was set to 0.3.

4.5 Qualitative Results

Fig. 6 shows qualitative comparisons of ETTrack and OC_SORT. The first row shows that OC_SORT causes ID switching owing to the object occlusion or non-linear motion. The Kalman Filter’s assumption of linear motion prevents OC_SORT from accurately predicting sudden pose changes, resulting in false matches. By contrast, ETTrack maintains consistent identities and exhibits robustness in handling non-linear motions. This demonstrates that our method can accurately predict the objects’ position when the objects exhibit complex and non-linear motions.



Fig. 7 The visualizations of ETTrack’s tracking results on the test set of SportsMOT and MOT17. Boxes of the same color denote the same object

The visualized results of ETTrack on the test set of SportsMOT and MOT17 are shown in Fig. 7. ETTrack provides accurate predictions on the test set of SportsMOT. It is demonstrated that our method can predict the positions of objects accurately in sports scenarios where the objects exhibit rapid and non-linear motions. Fig. 7 also shows several ETTrack’s tracking results on the test set of MOT17. It can be observed that although the MOT17 dataset is designed to track pedestrians in scenarios where motion patterns are generally linear, our method still delivers impressive tracking results.

5 Conclusion

In this paper, we propose a motion-based MOT called ETTrack, which uses an enhanced temporal motion predictor to improve object association and tracking performance in non-linear

motion. The motion predictor integrates a Temporal Transformer model and a Temporal Convolutional Network (TCN) to capture both local and global historical motion information. In addition, the proposed method uses a novel Momentum Correction Loss to guide the motion predictor during training and improve its ability to handle complex movements. As a result, compared to other motion models based on the Kalman Filter and deep learning, ETTrack exhibits better prediction performance on challenging datasets such as DanceTrack and SportsMOT. Simultaneously, it achieves comparable performance on pedestrian-centric datasets such as MOT17. In future work, we will conduct further research on camera motion information and human pose features in the motion model.

Funding The authors did not receive support from any organization for the submitted work.

Declarations

Conflict of interest Not applicable.

Data availability All datasets used are publicly available.

References

- Aharon N, Orfaig R, Bobrovsky BZ (2022) Bot-sort: Robust associations multi-pedestrian tracking. arXiv preprint arXiv:220614651
- Bai S, Kolter JZ, Koltun V (2018) An empirical evaluation of generic convolutional and recurrent networks for sequence modeling. arXiv preprint arXiv:180301271
- Bernardin K, Stiefelhagen R (2008) Evaluating multiple object tracking performance: the clear mot metrics. *EURASIP Journal on Image and Video Processing* 2008:1–10
- Bewley A, Ge Z, Ott L, et al. (2016) Simple online and realtime tracking. In: *2016 IEEE international conference on image processing (ICIP)*, IEEE, pp 3464–3468
- Cao J, Pang J, Weng X, et al. (2023) Observation-centric sort: Rethinking sort for robust multi-object tracking. In: *Proceedings of the IEEE/CVF conference on computer vision and pattern recognition*, pp 9686–9696
- Chaabane M, Zhang P, Beveridge JR, et al. (2021) Deft: Detection embeddings for tracking. arXiv preprint arXiv:210202267
- Choi W (2015) Near-online multi-target tracking with aggregated local flow descriptor. In: *Proceedings of the IEEE international conference on computer vision*, pp 3029–3037
- Chu P, Wang J, You Q, et al. (2023) Transmot: Spatial-temporal graph transformer for multiple object tracking. In: *Proceedings of the IEEE/CVF Winter Conference on applications of computer vision*, pp 4870–4880
- Cui Y, Zeng C, Zhao X, et al. (2023) Sportsmot: A large multi-object tracking dataset in multiple sports scenes. In: *Proceedings of the IEEE/CVF International Conference on Computer Vision*, pp 9921–9931
- Devlin J, Chang MW, Lee K, et al. (2018) Bert: Pre-training of deep bidirectional transformers for language understanding. arXiv preprint arXiv:181004805
- Du Y, Zhao Z, Song Y, et al. (2023) Strongsort: Make deepsort great again. *IEEE Transactions on Multimedia*
- Fischer T, Huang TE, Pang J, et al. (2023) Qdtrack: Quasi-dense similarity learning for appearance-only multiple object tracking. *IEEE Transactions on Pattern Analysis and Machine Intelligence*
- Ge Z, Liu S, Wang F, et al. (2021) Yolox: Exceeding yolo series in 2021. arXiv preprint arXiv:210708430
- Han S, Wang H, Yu E, et al. (2023) Ort: Occlusion-robust for multi-object tracking. *Fundamental Research*
- Kalman RE, et al. (1960) Contributions to the theory of optimal control. *Bol soc mat mexicana* 5(2):102–119
- Kesa O, Styles O, Sanchez V (2021) Joint learning architecture for multiple object tracking and trajectory forecasting. arXiv preprint arXiv:210810543
- Kingma D, Ba J (2014) Adam: A method for stochastic optimization. arXiv: Learning, arXiv: Learning
- Kuhn HW (1955) The hungarian method for the assignment problem. *Naval research logistics quarterly* 2(1-2):83–97
- Lan Z, Chen M, Goodman S, et al. (2019) Albert: A lite bert for self-supervised learning of language representations. arXiv preprint arXiv:190911942
- Lehmann EL, Casella G (2006) Theory of point estimation. *Springer Science & Business Media*
- Luiten J, Osep A, Dendorfer P, et al. (2021) Hota: A higher order metric for evaluating multi-object tracking. *International journal of computer vision* 129:548–578
- Luo W, Yang B, Urtasun R (2018) Fast and furious: Real time end-to-end 3d detection, tracking and motion forecasting with a single convolutional net. In: *Proceedings of the IEEE conference on Computer Vision and Pattern Recognition*, pp 3569–3577
- Meinhardt T, Kirillov A, Leal-Taixe L, et al. (2022) Trackformer: Multi-object tracking with transformers. In: *Proceedings of the IEEE/CVF conference on computer vision and pattern recognition*, pp 8844–8854

- Milan A, Leal-Taixé L, Reid I, et al. (2016) Mot16: A benchmark for multi-object tracking. arXiv preprint arXiv:160300831
- Milan A, Rezatofighi SH, Dick A, et al. (2017) Online multi-target tracking using recurrent neural networks. In: *Proceedings of the AAAI conference on Artificial Intelligence*
- Ristani E, Solera F, Zou R, et al. (2016) Performance measures and a data set for multi-target, multi-camera tracking. In: *European conference on computer vision*, Springer, pp 17–35
- Sun P, Cao J, Jiang Y, et al. (2012) Transtrack: Multiple object tracking with transformer. arXiv 2020. arXiv preprint arXiv:201215460
- Sun P, Kretzschmar H, Dotiwalla X, et al. (2020) Scalability in perception for autonomous driving: Waymo open dataset. In: *Proceedings of the IEEE/CVF conference on computer vision and pattern recognition*, pp 2446–2454
- Sun P, Cao J, Jiang Y, et al. (2022) Dance-track: Multi-object tracking in uniform appearance and diverse motion. In: *Proceedings of the IEEE/CVF Conference on Computer Vision and Pattern Recognition*, pp 20993–21002
- Vaswani A, Shazeer N, Parmar N, et al. (2017) Attention is all you need. *Neural Information Processing Systems, Neural Information Processing Systems*
- Wang Z, Zheng L, Liu Y, et al. (2020) Towards real-time multi-object tracking. In: *European conference on computer vision*, Springer, pp 107–122
- Wojke N, Bewley A, Paulus D (2017) Simple online and realtime tracking with a deep association metric. In: *2017 IEEE international conference on image processing (ICIP)*, IEEE, pp 3645–3649
- Wu J, Cao J, Song L, et al. (2021) Track to detect and segment: An online multi-object tracker. In: *Proceedings of the IEEE/CVF conference on computer vision and pattern recognition*, pp 12352–12361
- Xiao C, Cao Q, Zhong Y, et al. (2023) Motiontrack: Learning motion predictor for multiple object tracking. arXiv preprint arXiv:230602585
- Xu Y, Ban Y, Delorme G, et al. (2023) Transcenter: Transformers with dense representations for multiple-object tracking. *IEEE Transactions on Pattern Analysis & Machine Intelligence*
- Yuan Y, Iqbal U, Molchanov P, et al. (2022) Glamr: Global occlusion-aware human mesh recovery with dynamic cameras. In: *Proceedings of the IEEE/CVF conference on computer vision and pattern recognition*, pp 11038–11049
- Zagoruyko S, Komodakis N (2016) Wide residual networks. arXiv preprint arXiv:160507146
- Zeng F, Dong B, Zhang Y, et al. (2022) Motr: End-to-end multiple-object tracking with transformer. In: *European Conference on Computer Vision*, Springer, pp 659–675
- Zhang Y, Wang C, Wang X, et al. (2021) Fairmot: On the fairness of detection and re-identification in multiple object tracking. *International Journal of Computer Vision* 129:3069–3087
- Zhang Y, Sun P, Jiang Y, et al. (2022) Byte-track: Multi-object tracking by associating every detection box. In: *European conference on computer vision*, Springer, pp 1–21
- Zhang Y, Wang T, Zhang X (2023) Motrv2: Bootstrapping end-to-end multi-object tracking by pretrained object detectors. In: *Proceedings of the IEEE/CVF Conference on Computer Vision and Pattern Recognition*, pp 22056–22065
- Zhao Z, Chai W, Hao S, et al. (2023) A survey of deep learning in sports applications: Perception, comprehension, and decision. arXiv preprint arXiv:230703353
- Zhou X, Koltun V, Krähenbühl P (2020) Tracking objects as points. In: *European conference on computer vision*, Springer, pp 474–490
- Zhou X, Yin T, Koltun V, et al. (2022) Global tracking transformers. In: *Proceedings of the IEEE/CVF Conference on Computer Vision and Pattern Recognition*, pp 8771–8780
- Zhu X, Su W, Lu L, et al. (2020) Deformable detr: Deformable transformers for end-to-end object detection. arXiv preprint arXiv:201004159